International Journal of Solids and Structures 46 (2009) 2642–2649

Contents lists available at ScienceDirect

International Journal of Solids and Structures

journal homepage: www.elsevier.com/locate/ijsolstr

A procedure for estimating Young's modulus of textured polycrystalline materials

Masayuki Kamaya *

Institute of Nuclear Safety System, Inc., 64 Sata, Mihama-cho, Mikata-gun, Fukui 919-1205, Japan

ARTICLE INFO

Article history:
Received 24 September 2008
Received in revised form 13 February 2009
Available online 28 February 2009

Keywords:
Young's modulus
Elastic moduli
Polycrystalline aggregate
Anisotropic elasticity
Finite element analysis
Stainless steel
EBSD

ABSTRACT

In this study, a procedure for estimating Young's modulus of textured and non-textured polycrystalline materials was examined based on finite element analyses, which were performed using three-dimensional polycrystalline finite element models of a random structure, generated using the Voronoi tessellation. Firstly, the local stress/strain distribution and its influence on macroscopic elastic properties were evaluated. Then, the statistical relationship between Young's modulus obtained from the finite element analyses and averaged Young's modulus of all grains evaluated based on Voigt's or Reuss' model was investigated. It was revealed that the local stress/strain in the polycrystalline body is affected by crystal orientation and deformation constraint caused by adjacent grains, whereas only the crystal orientation affects Young's modulus of the polycrystalline body when the number of grains is large enough. It was also shown that Young's modulus correlates well with the averaged Young's modulus of all grains, in which the size of grains is considered in the averaging. Finally, a procedure for estimating Young's modulus of textured and non-textured materials was proposed. Young's modulus of various materials can be estimated from the elastic constants of single crystal and the distribution of crystal orientation and size of grains, which can be obtained by using electron backscatter diffraction (EBSD).

1. Introduction

Since a polycrystalline material is an aggregate of crystal grains of various sizes and shapes, its macroscopic properties are affected by the properties of individual grains. The elastic deformation of a single crystal exhibits anisotropy in most materials and depends on the orientation of the crystal. However, the macroscopic behavior of polycrystalline materials can be regarded as isotropic and homogeneous in terms of elastic deformation when the materials have random crystallographic and morphologic texture. The influence of the crystal orientation of individual grains on the elasticity of the aggregate is minor. Therefore, for engineering structural materials, we consider not the properties of individual grains but those of their aggregate, such as Young's modulus and Poisson's ratio.

However, this assumption may not be true when the material does not consist of a sufficient number of grains. Young's modulus of a micro-structure consisting of a small number of grains is dependent on the crystal orientations of individual grains in addition to the elasticity of a single crystal (Mullen et al., 1997; Nygårds, 2003). Even if the number of grains is large enough, Young's modulus is influenced by the crystal orientation of each grain for the textured material. In order to estimate Young's modulus of such structures, it is important to identify local properties, which are the elasticity and crystal orientation of each grain. Although it is difficult to identify the crystal orientations of all grains, a statistical distribution of crystal orientation can be obtained by using X-ray diffraction or electron backscatter diffraction (EBSD).

Once the crystal orientation of each grain or its statistical distribution is identified, Young's modulus of the aggregate can be evaluated by averaging Young's modulus of each grain (hereafter, local Young's modulus) based on a geometrical assumption. However, as explained in detail later, the geometrical condition (uniform local strain or stress) in a polycrystal is not obvious due to the complexity of the geometrical structure of a crystal grain. Furthermore, the complex geometry causes nonuniform stress at the microstructural level even under a uniform remote stress condition (Hashimoto and Margolin, 1983; Nichols et al., 1991; Sarma et al., 1998; Schroeter and McDowell, 2003; Kanit et al., 2003; Kamaya et al., 2007). The deformation constraint caused by neighboring grains as well as the variation in local Young's modulus induces large stress (or strain) near the grain boundary (Barbe et al., 2001; Diard et al., 2005; Kamaya, 2009). Such nonuniform stress may affect the macroscopic Young's modulus.

In order to quantify the effect of complex geometry and the local stress distribution in the polycrystalline material, it is necessary to use a numerical approach such as the finite element method. It has been shown that the local stress and strain distribution can be solved by using a reconstructed model of the grain structure and crystal orientations (Sumigawa et al., 2004; Zhao and Tryon, 2004; Lewis et al., 2005; Musienko et al., 2007; St-Pierre et al., 2008). Several attempts have been made to evaluate Young's

* Tel.: +81 770 379114; fax: +81 770 372009.
E-mail address: kamaya@inss.co.jp

0020-7683/$ - see front matter Æ 2009 Elsevier Ltd. All rights reserved.
doi:10.1016/j.ijsolstr.2009.02.013

modulus by elastic finite element analysis (FEA) by using polycrystalline models which were made by the Voronoi tessellation and of which crystal orientations were assigned randomly (Mullen et al., 1997; Chu et al., 2000; Nygårds, 2003; Sakaida and Sato, 2003; Serizawa et al., 2004). The FEA results showed reasonable Young's moduli, although they did not treat the textured material.

The objective of this study is to quantify the influence of texture on Young's modulus of the polycrystalline material. Three-dimensional polycrystalline finite element models of random structure were generated using the Voronoi tessellation. The local stress/strain distribution and its influence on elasticity were evaluated. Then, the statistical relationship between Young's modulus obtained from FEA and those from the averaged value of the local Young's modulus of all grains was investigated, and a procedure for estimating Young's modulus from the crystal orientations (or there distribution) was developed. The estimated Young's modulus was compared with the experimental results obtained using specimens of textured and non-textured materials. Finally, the procedure was generalized for various materials of different degree of anisotropy.

2. Procedure of analysis

2.1. Polycrystalline finite element models

Fig. 1 illustrates the geometry of the analyzed body of length L (=$2W$), width W, and thickness W. A uniform tensile load, P_o, was applied at the top and bottom of the body. In order to investigate the influence of deformation constraint, a bi-crystal model was made as shown in Fig. 2. Then, as shown in Fig. 3, random morphologic textured polycrystal models were generated by the Voronoi tessellation (Kitamura et al., 1993; Zhao and Tryon, 2004; Kamaya, 2004). The models consist of 16, 128, 432, 1024 and 2000 grains, and these are referred to as N16, N128, N432, N1024 and N2000, respectively. Each grain was divided into 8-nodes solid elements (in the bi-crystal model) or 4-nodes solid elements (in the other polycrystal models) by using the commercial mesh generator,

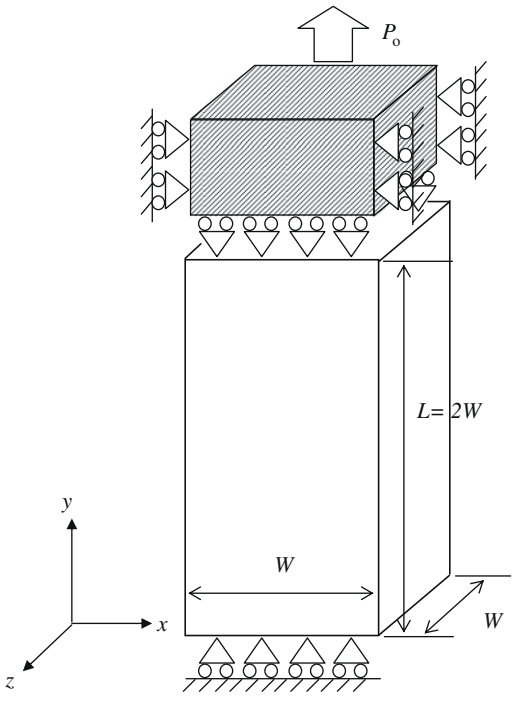

Fig. 1. Geometry and boundary condition of analyzed body.

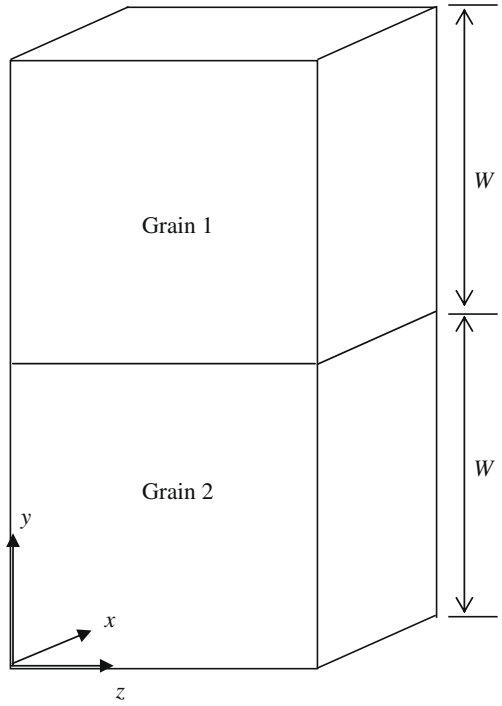

Fig. 2. Geometry of bi-crystal model.

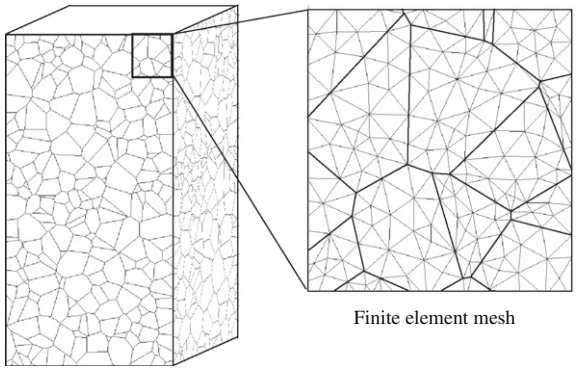

Fig. 3. Generated three-dimensional polycrystal model (number of grains: 2000).

PATRAN (PATRAN, 2007), in conjunction with an original programmed procedure. The mesh division was relatively fine near grain boundaries and their junction points. The total number of elements was 31,250, 9073, 26,225, 124,467, 231,694 and 1,448,324 for the bi-crystal, N16, N128, N432, N1024 and N2000 models, respectively.

2.2. Finite element analysis

Each grain was assumed to possess the anisotropic elasticity of cubic symmetry. The elastic constants used in this study are summarized in Table 1 (Ledbetter, 1981; Nagashima, 1984; Hosford, 1993). The constants for Type 316 stainless steel (SS) (Ledbetter, 1981) were mainly used except the cases for investigating the influence of material. Crystal orientations were determined randomly or chosen randomly from data groups, which were obtained from specimens of Type 316 stainless steel.

The general-purpose finite element solver ABAQUS, Version 6.5, (ABAUS, 2005) was employed for the elastic analyses. Young's modulus was derived from the displacement of the edge of the model, d_o, and denoted as E_{FEM}.

Table 1
Elastic constants used for analyses (GPa).

	C_{11}	C_{12}	C_{44}	Reference
Stainless steel (SS)	198	125	122	Ledbetter (1981)
Cu	168.4	121.4	75.4	Nagashima (1984)
Ni	246.5	147.3	124.7	Nagashima (1984)
Si	166.2	64.4	79.7	Hosford (1993)
Pb	49.5	42.3	14.9	Hosford (1993)

3. Young's modulus and crystal orientations of test specimens

Crystal orientations for the data group were obtained from specimens of Type 316 stainless steel. Five specimens were prepared, in which four specimens were made from the same material, but which exhibited different degrees of crystallographic texture depending on the sampling position. The alloying constituents and the texture of material are shown in Table 2. Crystal orientations were identified for each grain using EBSD. In many grains, the (1 0 0) plane is perpendicular to the loading axis. Crystal orientations of more than 5000 grains were measured for each of the five specimens and were recorded for each data group. The area of each grain was identified by counting the number of pixels in the crystal orientation map.

Young's modulus of the specimens was measured by strain gages and the results are shown in Table 2. The textured material showed a relatively small Young's modulus.

4. Young's modulus of aggregates

The elastic relationship between global strain $\{e_{(i)}\}$ and global stress $\{r_{(i)}\}$ of single crystal can be expressed as (Serizawa et al., 2004)

$$\{r_{(i)}\} = [T_{(i)}]^{-1}[C][T_{(i)}]\{e_{(i)}\}, \tag{1}$$

where $[C]$ is the stiffness matrix and $[T_{(i)}]$ represents the transform matrix of the stiffness from the global coordinate system to the crystal one of grain i, and is calculated by the crystal orientation. Young's modulus of an aggregate of grains can be obtained by averaging the elasticity of all grains. However, it is not obvious how to perform this averaging for a polycrystalline material. The following two extreme methods have been proposed (Voigt, 1928; Reuss, 1929). Voigt's model assumes uniform local strains. Based on this assumption, the averaged stiffness $[C]_V$ can be obtained as

$$[C]_V = \frac{1}{V_o}\sum_{i}^{N_g} V_{(i)}[T_{(i)}]^{-1}[C][T_{(i)}], \tag{2}$$

where $V_{(i)}$ denotes the volume of grain i, and V_o is the total volume of the polycrystalline body whose number of grains is N_g. On the other hand, Reuss' model assumed uniform local stress, therefore, the compliances can be averaged for each grain. The averaged compliance $[S]_R$ is obtained by

$$[S]_R = \frac{1}{V_o}\sum_{i}^{N_g} V_{(i)}[T_{(i)}]^{-1}[C]^{-1}[T_{(i)}]. \tag{3}$$

Table 2
Chemical contents and measured Young's moduli of test specimens.

Specimen	Young's modulus (GPa)	Chemical content (wt%)
TS1	147	0.016C, 0.37Si, 1.46Mn, 0.030P, 0.001S, 11.69Ni, 17.31Cr, 2.12Mo and balance in Fe
TS2	159	
TS3	151	
TS4	156	
NT1	198	0.021C, 0.49Si, 1.39Mn, 0.032P, 0.025S, 12.11Ni, 17.14Cr, 2.05 Mo and balance in Fe

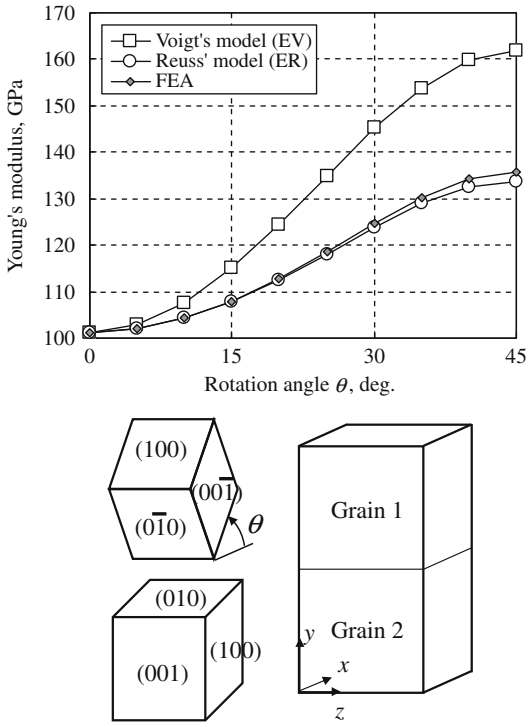

Fig. 4. Change in Young's modulus with rotation angle of Grain 1.

Young's modulus can be evaluated from the global deformation of the aggregate obtained using the stiffness $[C]_V$ and compliance $[S]_R$. Young's modulus obtained from Voigt's model (E_V) and that from Reuss' model (E_R) give the upper and lower bounds to the true value, respectively (Hosford, 1993).

5. Results and discussion

5.1. The bi-crystal model

Fig. 4 shows the change in Young's modulus of the bi-crystal model with the rotation angle of Grain 1. Grain 1 was rotated from the (1 0 0) plane to (1 1 0) plane with respect to the loading axis, whereas Grain 2 was fixed to the (1 0 0) plane. The elastic constants of SS were used. Since the grain structure of the bi-crystal model is the same as that of Reuss' model, the change in Young's modulus (E_{FEM}) was almost identical to E_R. However, E_{FEM} is not exactly the same as E_R. Fig. 5 shows the stress (r_{22}) and strain (e_{22}) near the surface of the body when $h = 4\bar{5}$. Here, the stress and strain were obtained by interpolating adjacent integral points of the solid elements, and normalized by the macroscopic value $r_o(=P_o/W^2)$ and $e_o(=d_o/L)$, respectively. According to Reuss' assumption, the stress should be the same in the entire body. However, some variation in stress was observed, although the magnitude of variation was much smaller than that of strain. The deformation constraint between the grains causes deviation from the ideal Reuss' model and variation of the stress and strain near the grain boundary. The magnitude of the difference between E_{FEM} and E_R is much smaller than the change in Young's modulus caused by the rotation of Grain 1.

5.2. Stress and strain distributions in polycrystal models

Fig. 6 shows the change in stress (r_{22}) and strain (e_{22}) along a line parallel to the loading axis in models N16 and N128. Crystal orientations were assigned randomly and the elastic constants of SS were used. In the polycrystalline body, both of Voigt's and Reuss' model are not appropriate due to the complexity of grain

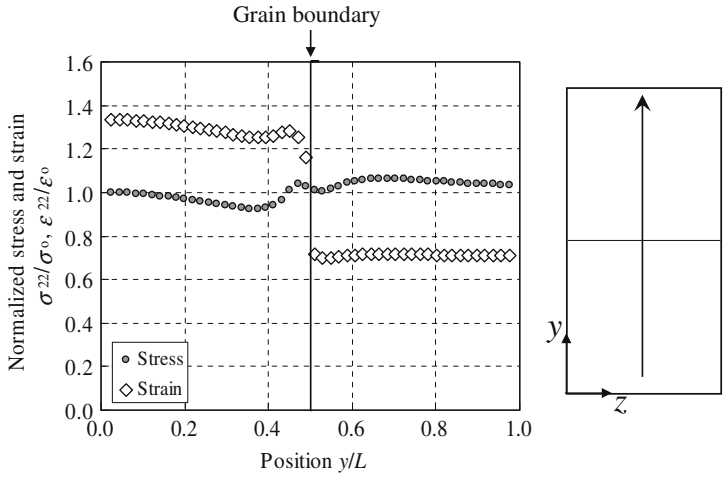

Fig. 5. Normalized stress (r_{22}/r_o) and strain (e_{22}/e_o) along a line on the surface (bi-crystal model).

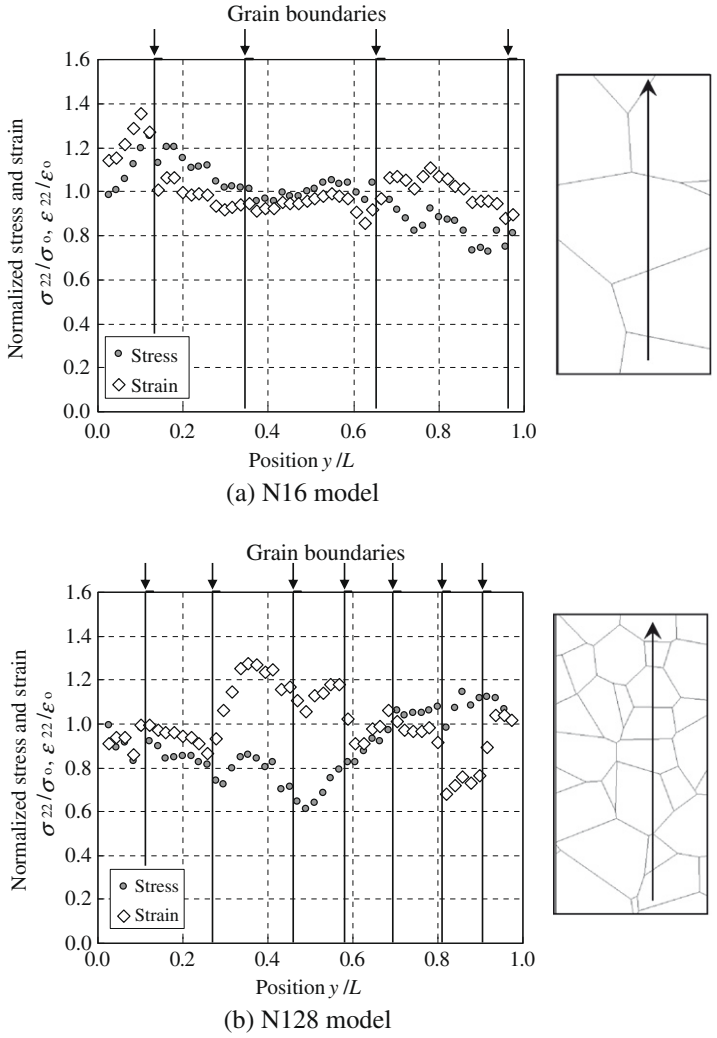

Fig. 6. Normalized stress (r_{22}/r_o) and strain (e_{22}/e_o) along a line on the surface (polycrystal models).

structure. The extent of variation of the stress and strain was similar, and this means that neither of Voigt's and Reuss' models is predominant in the polycrystalline body.

The stress and strain tended to vary grain by grain. This suggests that the stress (strain) in the grain is governed primarily by crystal orientation. This can be confirmed by Fig. 7, which shows the relationship between the local Young's modulus for each grain and the averaged stress and strain. The local Young's modulus was calculated from the stiffness matrix in the global coordinate system ($[T_{(i)}]^{-1}[C][T_{(i)}]$) of each grain, and the averaged stress and

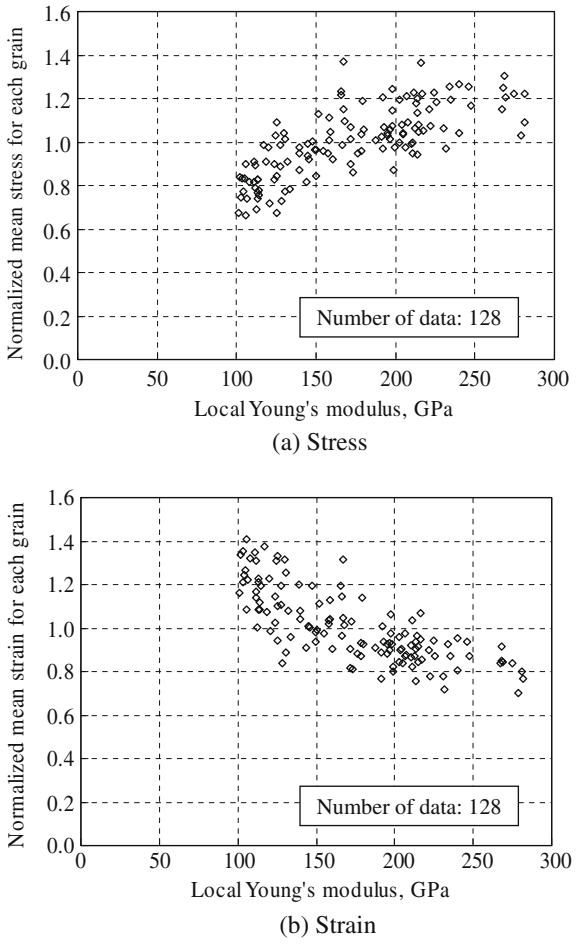

Fig. 7. Relationship between Young's modulus of each grain and averaged values of stress and strain (N128 model).

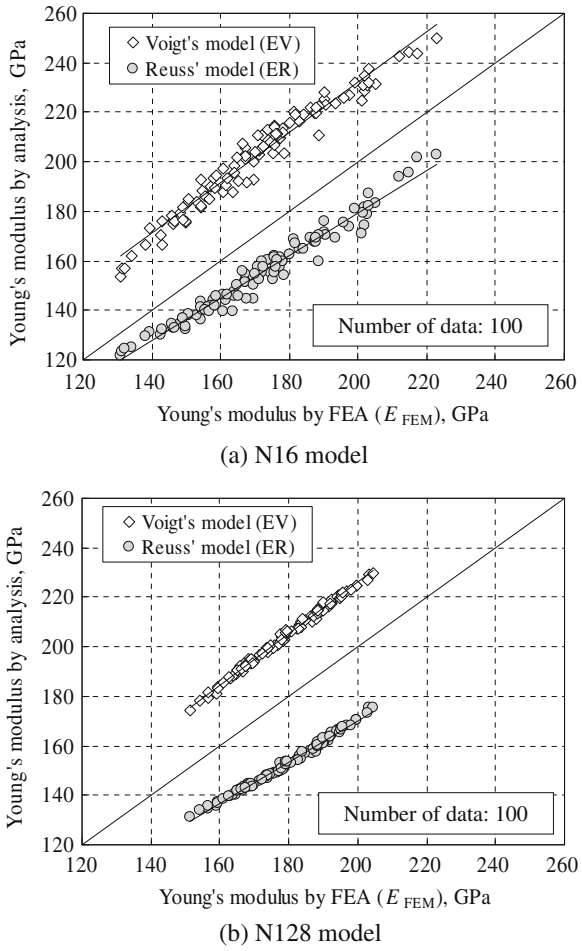

Fig. 8. Comparison of Young's moduli obtained by FEA and by estimation (crystal orientations are obtained from textured materials).

strain were the average of all elements in the grain. Both of the strain and stress exhibit correlation with the local Young's modulus. Therefore, it is expected that the macroscopic deformation (d_o) correlates with the average of the local Young's modulus such as E_V and E_R. Note that a clear correlation could not be found between the local Young's modulus and grain size.

The stress and strain varied significantly inside some grains due to the deformation constraint caused by adjacent grains, and this variation might have affected the Young's modulus.

5.3. Young's modulus of polycrystalline body

The relationship between Young's moduli obtained by FEA (E_{FEM}) and those estimated by Voigt's (E_V) and Reuss' models (E_R) is shown in Fig. 8. This figure includes 100 results obtained using 20 combinations of crystal orientation that were selected randomly from each data group. Due to differences of the degree of crystallographic texture of specimens and the combinations of crystal orientations, Young's moduli showed large variations, and the range of variation of the N16 model was larger than that of the N128 model. The effect of local Young's modulus of each grain on Young's modulus is larger for the model with fewer grains.

In spite of large variation, E_V and E_R correlate well with E_{FEM}, and form the upper and lower limits of E_{FEM}, respectively. This implies that Young's modulus of the polycrystalline body greatly depends on the combinations of crystal orientations. The ambiguousness of the geometrical condition (uniform local strain or uniform local stress) and the deformation constraint also affects Young's modulus in the polycrystalline body, although it seems to bring about a relatively small effect. In the N16 model, E_{FEM} is nearer to E_R rather than E_V. The polycrystalline model is a rectangular parallelepiped and longer in the loading direction. Therefore, the model tends to satisfy the uniform local stress condition (Reuss' model) statistically. This effect is reduced as the number of grains increases.

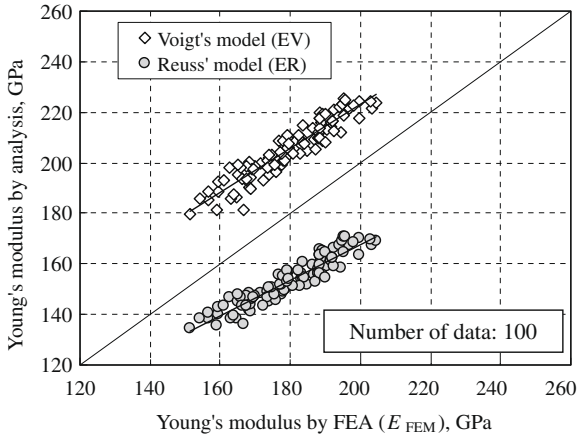

Fig. 9. Comparison of Young's moduli obtained by FEA and by estimation (FEA results is the same as Fig. 8(b), whereas uniform grain size is assumed for E_V and E_R) (N128 model).

In Fig. 9, E_V and E_R were evaluated assuming that the volume of grains was the same for all grains, whereas the results of FEA were the same as shown in Fig. 8(b). The correlation becomes worse than that of Fig. 8(b), implying that it is important to consider the volume of grains for the estimation of Young's modulus by Eqs. (2) and (3).

Fig. 10 shows the change in averaged deviation of E_{FEM} from the regression line. An increase in the number of grains enhances the averaging effect and reduces the effect of the geometrical condition and the deformation constraint. As the number of grains increases, Young's modulus of the polycrystalline aggregate appears to be determined by the combination of the crystal orientations of the grains and their size. The averaged error from the regression line is less than 0.3 GPa when the number of grains is more than 1024.

5.4. Estimation of Young's modulus of stainless steel

Since E_{FEM} correlates well with E_R and E_V in a polycrystalline body of a large number of grains, by evaluating the correlation it is possible to estimate Young's modulus of the material from E_R or E_V quantitatively. By using the N1024 model, the correlation was obtained from 1000 calculations using 200 combinations of crystal orientation for each data group as shown in Fig. 11. E_{FEM} correlates fairly well with E_R and E_V, and a linear regression leads to the following equations:

$$E_{FEA} = 1.00E_V - 21.5, \quad (4)$$

$$E_{FEA} = 1.21E_R - 2.17. \quad (5)$$

The inclination of the regression line is almost unity for Voigt's model, whereas it is 1.2 for Reuss' model. E_{FEM} tended to be close to E_R for a small Young's modulus as shown in Fig. 8. Since Eq. (4) is easier to treat, Young's modulus was estimated by

$$E_{est} = E_V - 21.5, \quad (6)$$

where E_{est} is the estimated Young's modulus.

By using Eq. (6), Young's modulus of each specimen was estimated using 2000 crystal orientations in each data group. In the measurement of crystal orientations of the specimens, the area of grains at the observed surface was identified in addition to the crystal orientation. The 1.5th power of area was used as $V_{(i)}$ for the calculation of E_V by Eq. (2). Fig. 12 compare the estimated Young's modulus and the experimental results. These values agree well, suggesting that the current estimation procedure is valid. In other words, the difference in Young's modulus between the specimens can be explained by the crystallographic texture. In spite of large variations in Young's modulus due to texture, it could be estimated by measuring the orientation and size of crystals by using EBSD.

5.5. Estimation of Young's modulus of various materials

The estimation of Young's modulus using Eq. (6) is valid only for stainless steel. In order to apply this estimation procedure to various materials, the correlation was investigated for several materials, which are listed in Table 1. By using the N1024 model, the correlation was obtained from 1000 calculations using 200 combinations of crystal orientation for each data group as was done for Fig. 11. Fig. 13 shows the obtained correlation, where the parameter for anisotropy of elasticity was defined by the equation:

$$A = \frac{2C_{44}}{C_{11} - C_{12}}, \quad (7)$$

where a denotes a parameter representing the correlation defined by

$$E_{est} = E_V - \frac{a}{E_{Vo}}, \quad (8)$$

where E_{Vo} is Young's modulus of a non-textured material calculated by Hosford (1993)

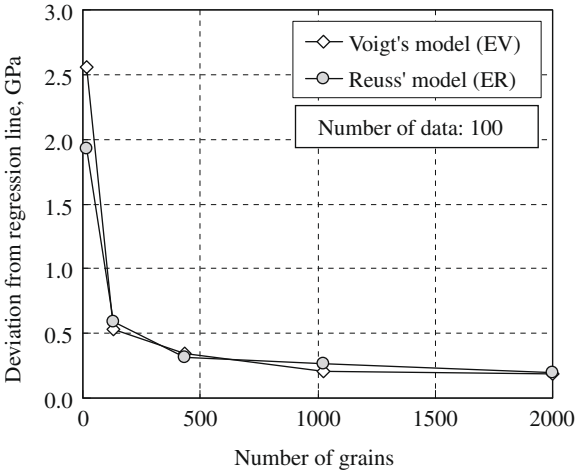

Fig. 10. Change in deviation of Young's modulus from regression line with number of grains in polycrystalline body.

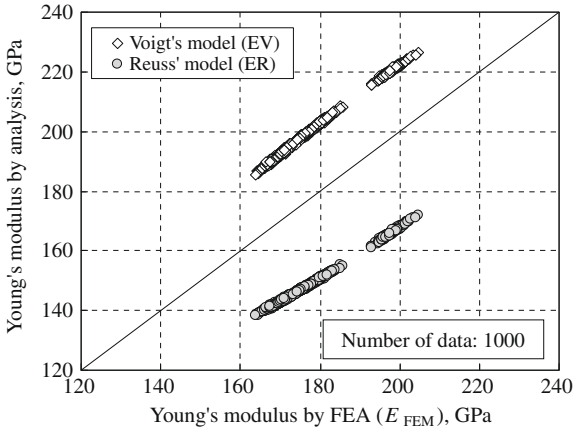

Fig. 11. Comparison of Young's moduli obtained by FEA and by estimation (N1024 model).

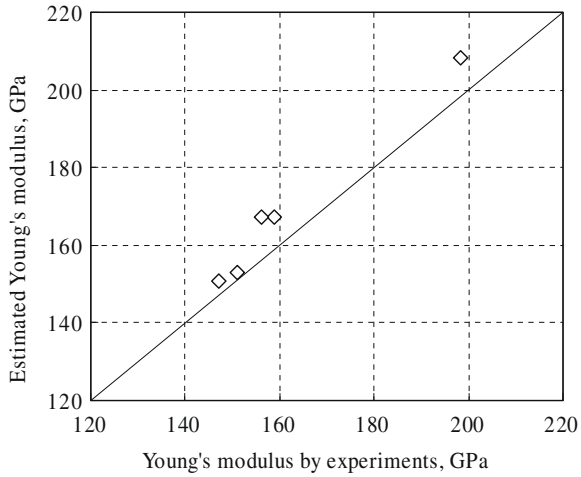

Fig. 12. Comparison of Young's moduli by experiment and by estimation.

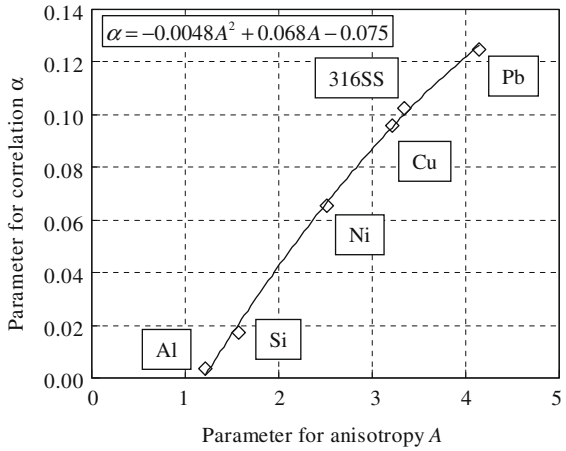

Fig. 13. Relationship between the parameter for anisotropy (A) and the parameter for correlation (a).

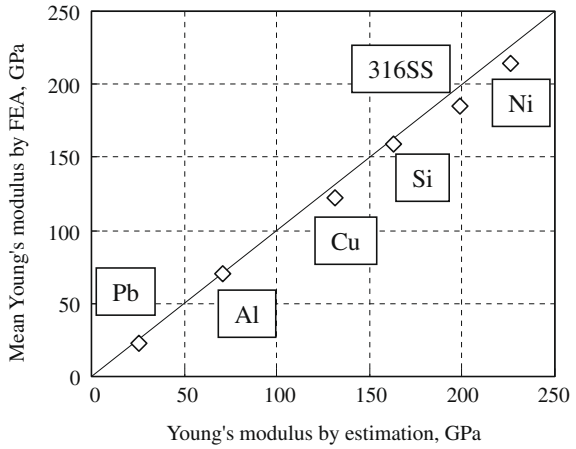

Fig. 14. Relationship between averaged Young's moduli by finite element analysis for 1000 cases and estimated Young's moduli for non-textured material.

$$E_{\mathrm{Vo}} = \frac{(c_{11} - c_{12} + 3c_{44})(c_{11} + 2c_{12})}{2c_{11} + 3c_{12} + c_{44}}. \tag{9}$$

As shown in Fig. 13, the parameters A and a show good correlation and the regression curve was obtained as

$$a = -0.0048A^2 + 0.068A - 0.075. \tag{10}$$

Once E_{V} of the material is evaluated, we can estimate Young's modulus of a textured material using the elastic constants of a single crystal.

When the crystallographic texture of the material is weak enough, the crystal orientations can be regarded as distributed uniformly and E_{V} can be evaluated as the average of all orientations. Eq. (9) for E_{Vo} was derived for a non-textured material assuming that the sizes of grains are the same. Fig. 14 shows the relationship between the estimated Young's modulus, which was evaluated by substituting $E_{\mathrm{V(eqi)}}$ for E_{V} in Eq. (8), and those obtained by FEA, which were performed 1000 times for different combinations of crystal orientation determined randomly. The agreement of these values implies that the current estimation procedure can be applied not only to textured materials but also to non-textured materials.

6. Summary and conclusions

In order to quantify the influence of crystallographic texture on Young's modulus of polycrystalline materials, three-dimensional polycrystal models were analyzed by the finite element method. Factors that control Young's modulus of the polycrystalline aggregate were examined and a procedure for estimating Young's modulus of textured and non-textured materials was proposed. The results are summarized as follows:

(1) Young's modulus is influenced by three factors, which are the crystal orientation, deformation constraint and geometrical condition (uniform local stress or strain), whereas only the crystal orientation is relevant to the estimation of Young's modulus when the number of grains is large enough.
(2) Young's modulus correlates well with the estimated value based on Voigt's or Reuss' model, in which the size of grain is considered.
(3) By using the proposed procedure, Young's modulus of textured and non-textured materials can be estimated from the elastic constants of a single crystal and the distribution of crystal orientation and size of grains, which can be obtained by using EBSD.

References

ABAUS, 2005. ABAQUS User's manual Version 6.5, ABAQUS Inc.
Barbe, F., Forest, S., Cailletaud, G., 2001. Intergranular and intragranular behavior of polycrystalline aggregates. Part 2. Results. International Journal of Plasticity 17, 537–563.
Chu, Z., Mullen, R.L., Ballarini, R., 2000. Statistical properties of elastic moduli of polycrystalline materials using a Johnson–Mehl model. In: Proceedings of the 8th ASCE Specialty Conference on Probabilistic Mechanics and Structural Reliability, Indiana.
Diard, O., Leclercq, S., Rousselier, G., Cailletaud, G., 2005. Evaluation of finite element based analysis of 3D multicrystalline aggregates plasticity: application to crystal plasticity model identification and the study of stress and strain fields near grain boundaries. International Journal of Plasticity 21, 691–722.
Hashimoto, K., Margolin, H., 1983. The role of elastic interaction stresses on the onset of slip in polycrystalline alpha brass – II. Rationalization of slip behavior. Acta Metallurgica 31 (5), 787–800.
Hosford, W.F., 1993. The Mechanics of Crystals and Textured Polycrystals. Oxford University Press, Oxford.
Kamaya, M., 2004. Influence of grain boundaries on short crack growth behaviour of IGSCC. Fatigue & Fracture of Engineering Materials & Structures 27, 513–521.
Kamaya, M., 2009. Measurement of local plastic strain distribution of stainless steel by electron backscatter diffraction. Material Characterization 60, 125–132.
Kamaya, M., Kawamura, Y., Kitamura, T., 2007. Three-dimensional local stress analysis on grain boundaries in polycrystalline material. International Journal of Solids and Structures 44, 3267–3277.
Kanit, T., Forest, S., Galliet, I., Mounoury, V., Jeulin, D., 2003. Determination of the size of the representative volume element for random composites: statistical and numerical approach. International Journal of Solids and Structures 40, 3647–3679.
Kitamura, T., Tada, N., Ohtani, R., 1993. Evaluation of creep fatigue damage based on initiation and growth of small cracks. In: Behavior of Defects at High Temperatures, ESIS 15, Mechanical Engineering Publications, pp. 47–69.
Ledbetter, H.M., 1981. Predicted single-crystal elastic constants of stainless-steel 316. British Journal of Non-Destructive Testing 23, 286–287.
Lewis, A.C., Bingert, J.F., Rowenhorst, D.J., Gupta, A., Geltmacher, A.B., Spanos, G., 2005. Two- and three-dimensional microstructural characterization of a super-austenitic stainless steel. Materials Science and Engineering Part A 418 (1–2), 11–18.
Mullen, R.L., Ballarini, R., Yin, Y., Heuer, A.H., 1997. Monte Carlo simulation of effective elastic constants of polycrystalline thin films. Acta Materialia 45 (6), 2247–2255.
Musienko, A., Tatschl, A., Schmidegg, K., Kolednik, O., Pippan, R., Cailletaud, G., 2007. Three-dimensional finite element simulation of a polycrystalline copper specimen. Acta Materialia 55, 4121–4136.
Nagashima, S., 1984. Sugososhiki. Maruzen, Tokyo (in Japanese).
Nichols, C.S., Cook, R.F., Clarke, D.R., Smith, D.A., 1991. Alternative length scales for polycrystalline materials. Acta Metallurgica et Materialia 39, 1657–1665.
Nygårds, M., 2003. Number of grains necessary to homogenize elastic materials with cubic symmetry. Mechanics of Materials 35, 1049–1057.
PATRAN, 2007. MSC/PATRAN 2007 User's Manual, MSC Software Corp.
Reuss, A., 1929. Mathematics and Mechanics 9, 49–58.
Sakaida, Y., Sato, K., 2003. Prediction of homogenized elastic moduli of ceramics using polycrystalline grain model. Transactions of the Japan Society of Mechanical Engineers 69 (684), 1311–1317.
Sarma, G.B., Radhakrishnan, B., Zacharia, T., 1998. Finite element simulations of cold deformation at the mesoscale. Computational Materials Science 12, 105–123.

Schroeter, B.M., McDowell, D.L., 2003. Measurement of deformation fields in polycrystalline OFHC copper. International Journal of Plasticity 19 (9), 1355–1376.

Serizawa, K., Tanaka, K., Kimachi, H., Akiniwa, Y., 2004. Finite element analysis of elastic deformation of cubic polycrystalline thin films with ⟨001⟩ fiber texture. Journal of the Society of Materials Science, Japan 53 (2), 150–156.

St-Pierre, L., Héripré, E., Dexet, M., Crépin, J., Bertolino, G., Bilger, N., 2008. 3D Simulations of microstructure and comparison with experimental microstructure coming from O.I.M analysis. International Journal of Plasticity 24, 1516–1532.

Sumigawa, T., Kitamura, T., Ohishi, K., 2004. Slip behaviour near a grain boundary in high-cycle fatigue of poly-crystal copper. Fatigue & Fracture of Engineering Materials & Structures 27, 495–503.

Voigt, W., 1928. Lehrbuch der Kristalphysik. Teubner, Berlin.

Zhao, Y., Tryon, R., 2004. Automatic 3-D simulation and micro-stress distribution of polycrystalline metallic materials. Computer Methods in Applied Mechanics and Engineering 193, 3919–3934.